

***NANOSCALE NMR STUDIES OF
TOPOLOGICAL INSULATORS,***

**CRYSTALLINE INSULATORS AND
DIRAC SEMIMETALS**

Louis Bouchard

UCLA

Mar. 22, 2019

TODAY'S TOPICS

Topological band structures

Topological Insulators

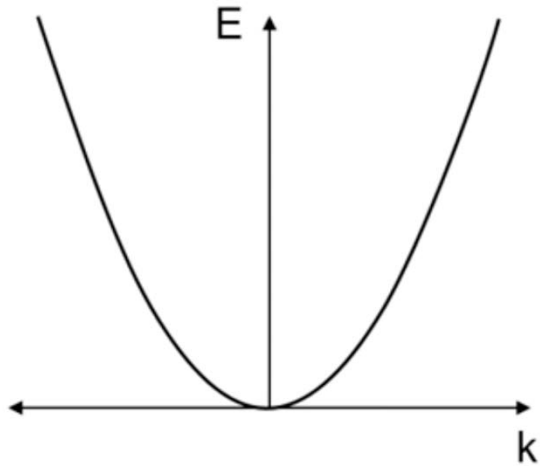
Topological Crystalline Insulators

Dirac Semimetals

Electrons In Crystals

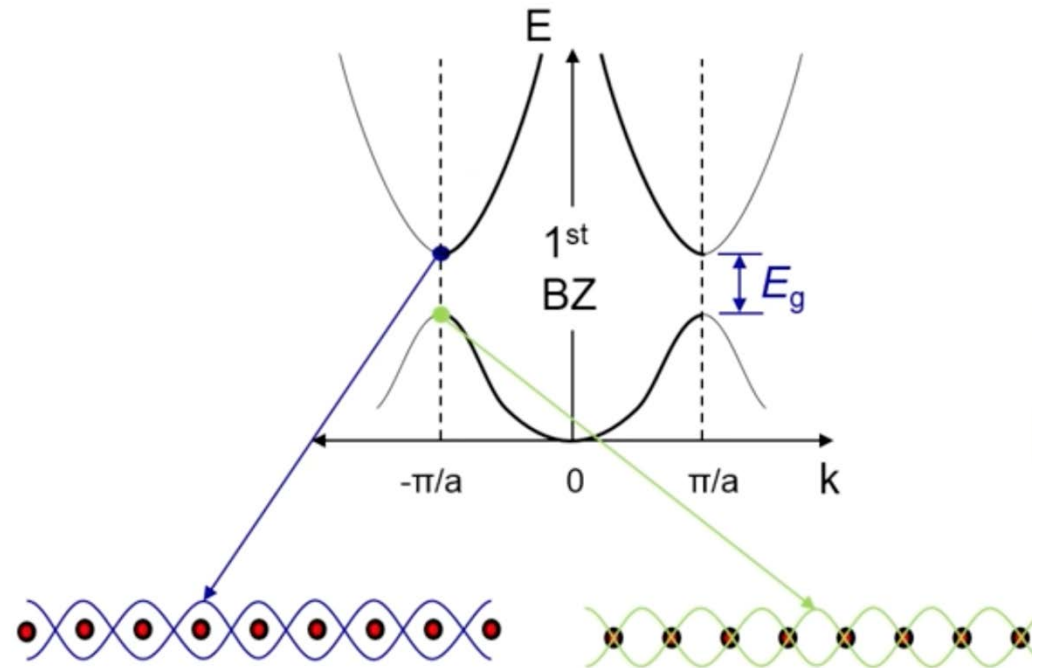
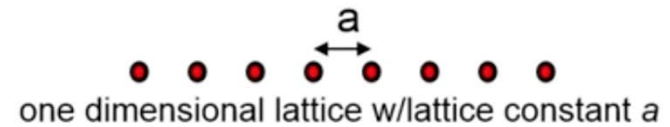
Electrons are waves

Free electrons



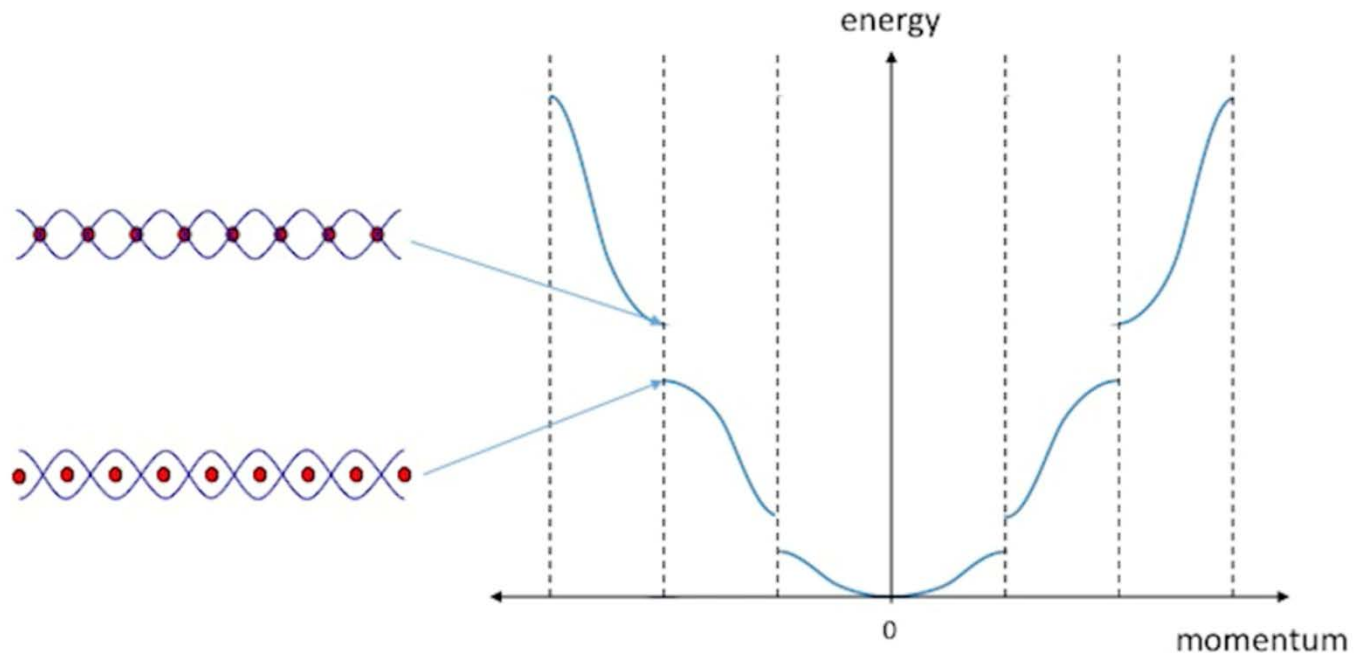
$$H = \frac{\hbar^2 k^2}{2m}$$

Nearly free electrons



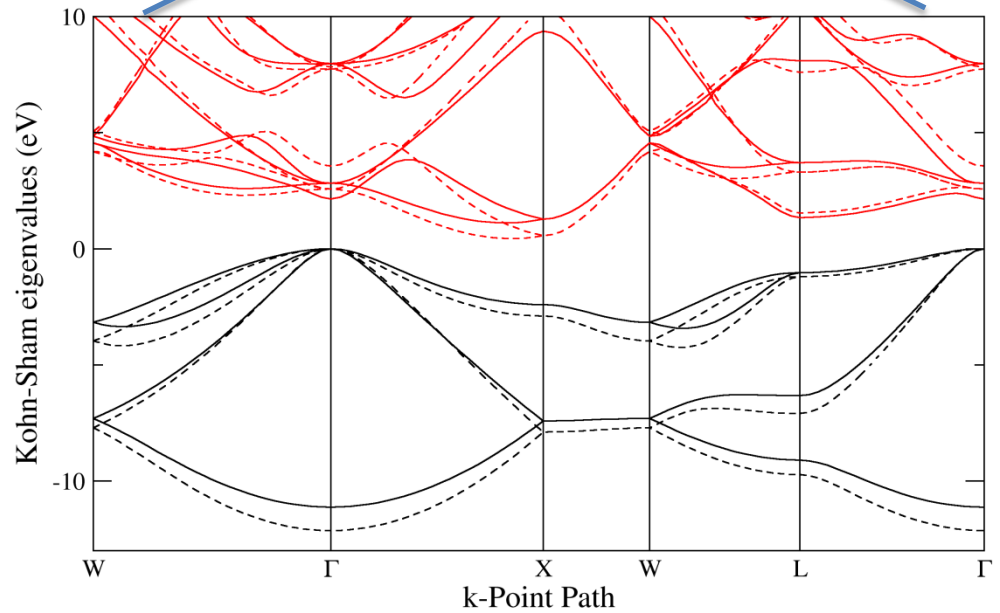
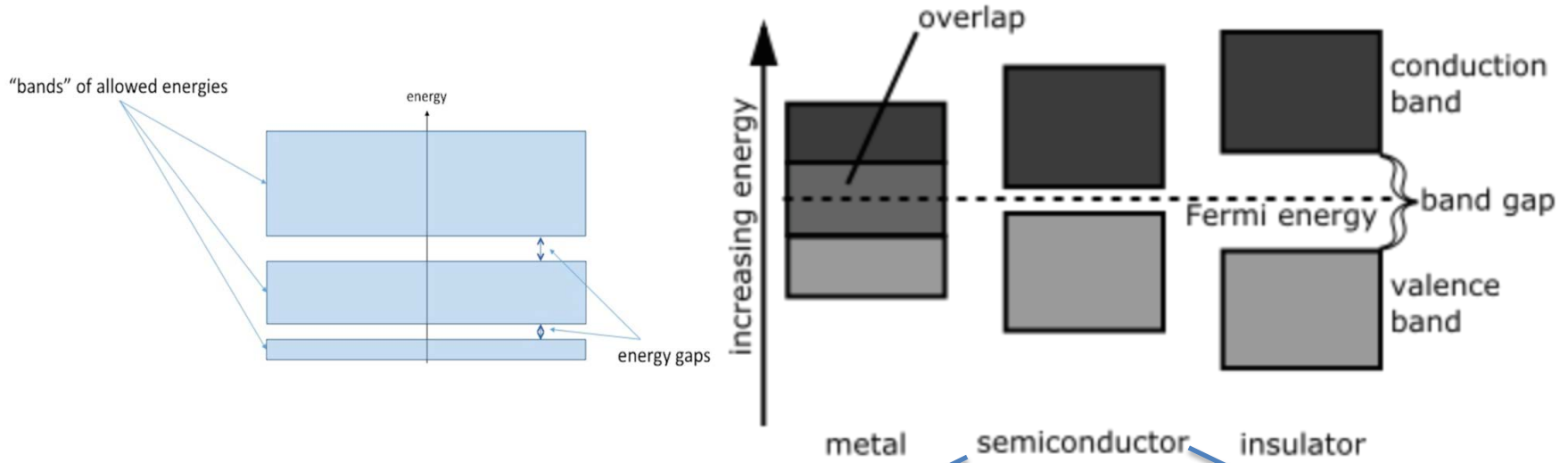
Things happen when $e^{-} k =$ lattice spacing

Electrons In Crystals: Things Happen When $e^- k =$ Lattice Spacing



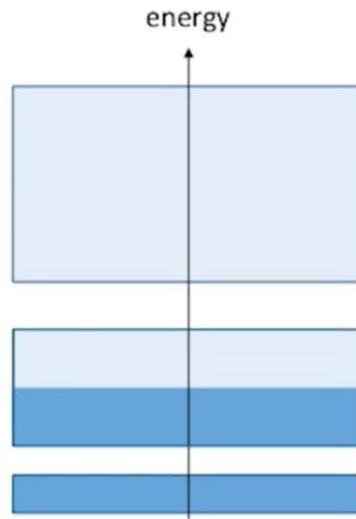
e^- like to be on top of atoms (lowers energy),
but not in between (higher energy)

Band Theory of Solids

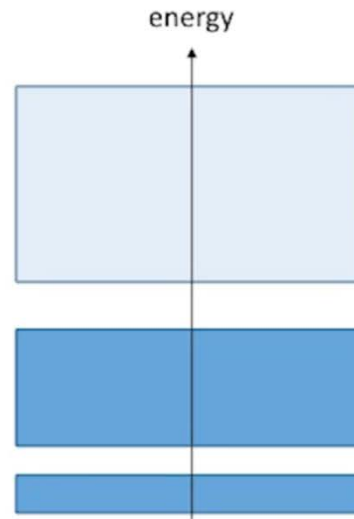


Si

Macroscopic Solid: Add e⁻ Fills Bands



metal:
conducts electricity

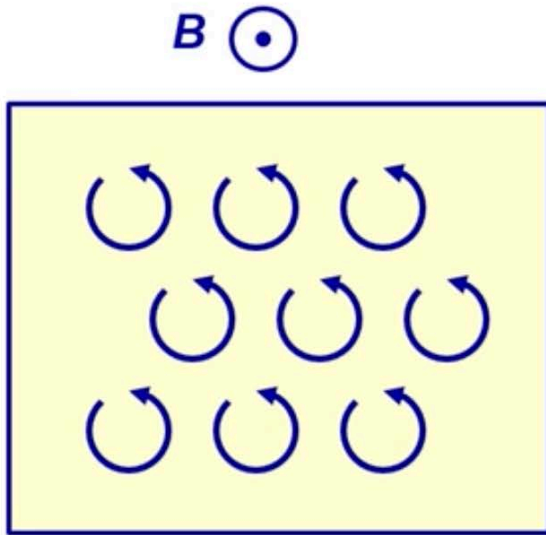


insulator:
doesn't conduct electricity



Insulators: e⁻ move around but no net movement

2D Metal in Magnetic Field



$$\left[\frac{(\mathbf{p} + e\mathbf{A})^2}{2m} \right] \Psi = E\Psi$$

$$\mathbf{A} = By\hat{\mathbf{x}}$$

$$\left[\frac{(p_x + eBy)^2}{2m} + \frac{p_y^2}{2m} \right] \Psi = E\Psi$$

$$\Psi = e^{ik_x x} \chi(y)$$

$$\left[\frac{p_y^2}{2m} - \frac{1}{2} m\omega_c^2 (y + y_k)^2 \right] \chi(y) = E\chi(y)$$

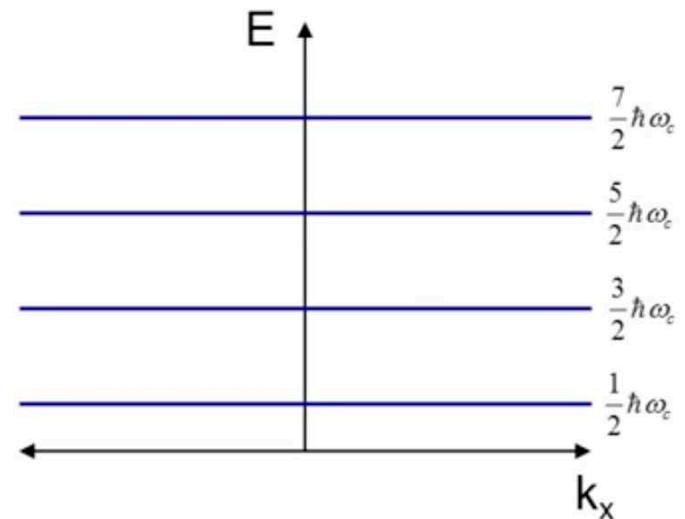
Solutions are harmonic oscillators

Localized in space, $v_{\text{group}} = 0$

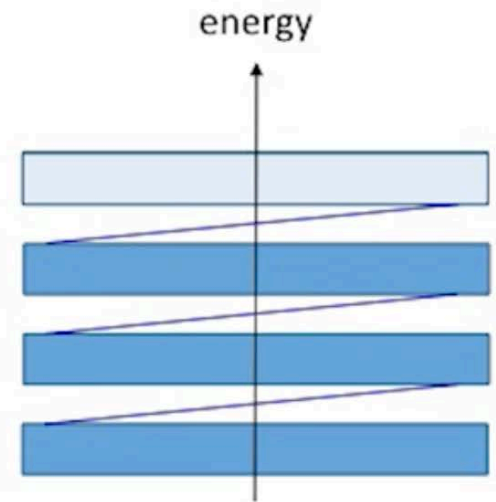
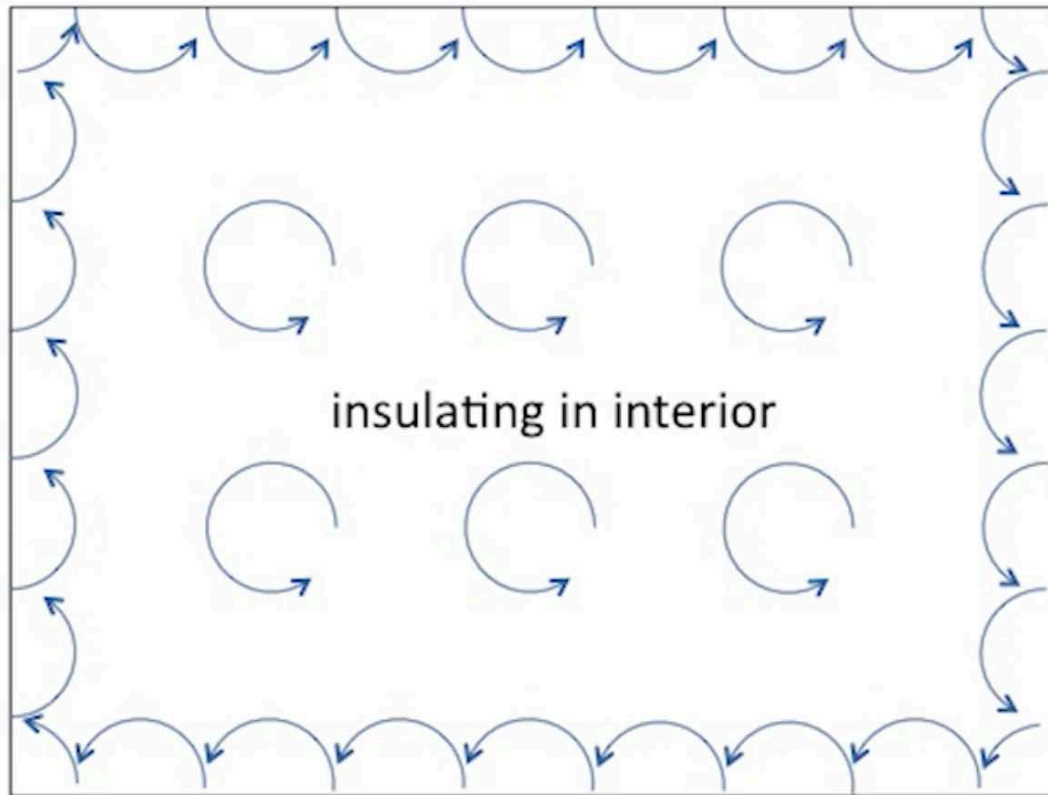
Highly degenerate with discrete energies:

$$E = \left(n + \frac{1}{2} \right) \hbar\omega_c \quad \omega_c = \frac{eB}{m}$$

“Landau levels”

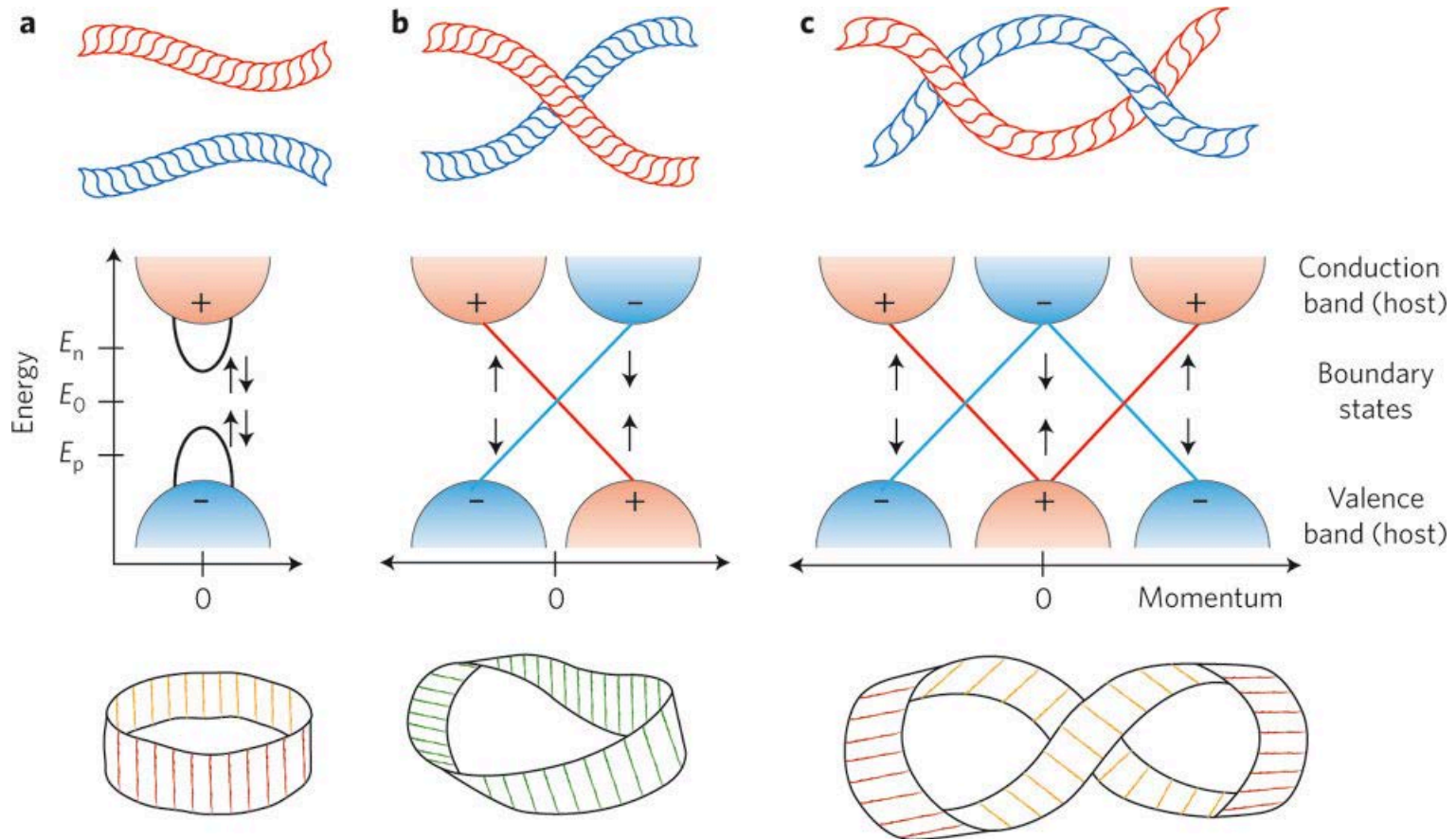


Topology: 1D Edge States Conduct Current



Boundaries are perfect conductors – no resistance

TI & Topological Invariant



H.C. Manoharan, Nature Nanotechnology 5, 477–479 (2010)

TKNN: Topological Invariant for QHE

Berry connection

$$\mathbf{A}(\mathbf{k}) = -i \langle u_i(\mathbf{k}) | \nabla_{\mathbf{k}} | u_i(\mathbf{k}) \rangle$$

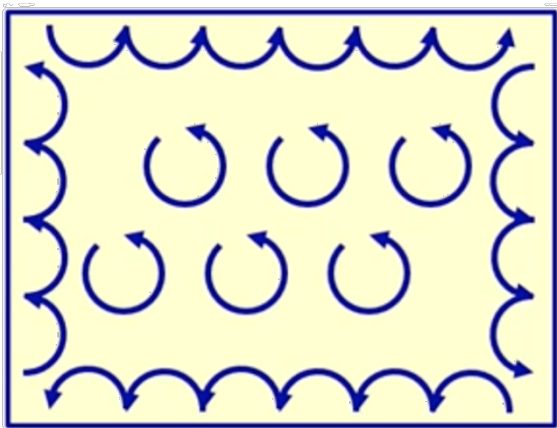
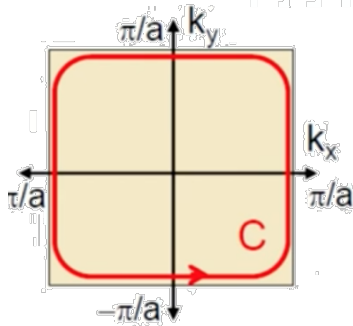
Berry curvature

$$\mathbf{F}(\mathbf{k}) = \nabla_{\mathbf{k}} \times \mathbf{A}(\mathbf{k})$$

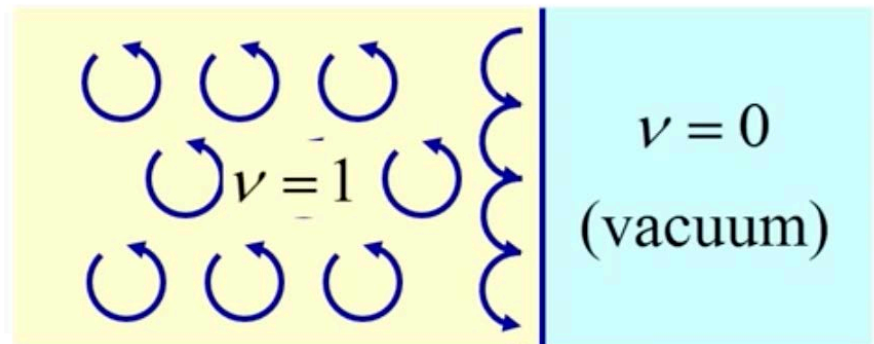
TKNN invariant

$$\nu = \frac{1}{2\pi} \oint_C \mathbf{A}(\mathbf{k}) \cdot d\mathbf{k} = \frac{1}{2\pi} \int_{BZ} \mathbf{F}(\mathbf{k}) d^2\mathbf{k}$$

$$\sigma = \begin{pmatrix} 0 & -\nu \frac{e^2}{h} \\ \nu \frac{e^2}{h} & 0 \end{pmatrix}$$

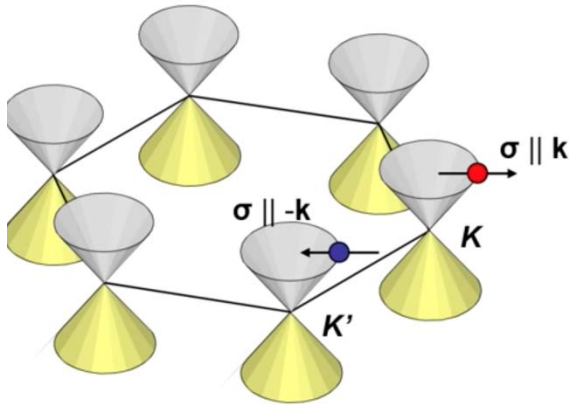


Edge-State Picture of QHE



of chiral modes = $\Delta\nu$

Are Landau levels the only system with TKNN $\nu \neq 0$?



$$\hbar v_F \begin{pmatrix} 0 & k_x - ik_y \\ k_x + ik_y & 0 \end{pmatrix} \begin{pmatrix} F_A(r) \\ F_B(r) \end{pmatrix} = \varepsilon \begin{pmatrix} F_A(r) \\ F_B(r) \end{pmatrix}$$

$$\hbar v_F (\boldsymbol{\sigma} \cdot \mathbf{k}) F(r) = \varepsilon F(r)$$

$$|k\rangle = \frac{1}{\sqrt{2}} \underbrace{e^{i\mathbf{k} \cdot \mathbf{r}}}_{\text{Plane wave}} \underbrace{\begin{pmatrix} -ibe^{-i\theta_k/2} \\ e^{i\theta_k/2} \end{pmatrix}}_{\text{spinor}}$$

Plane wave

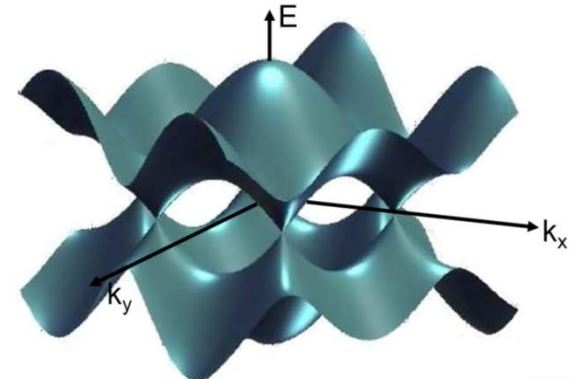
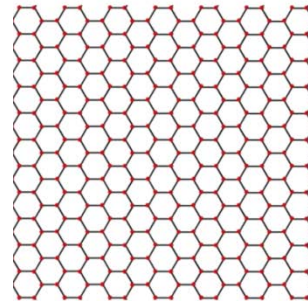
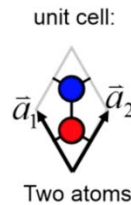
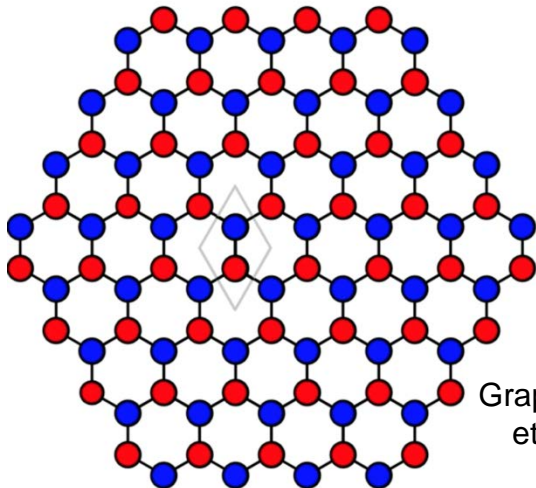
spinor

Two identical atoms in unit cell:



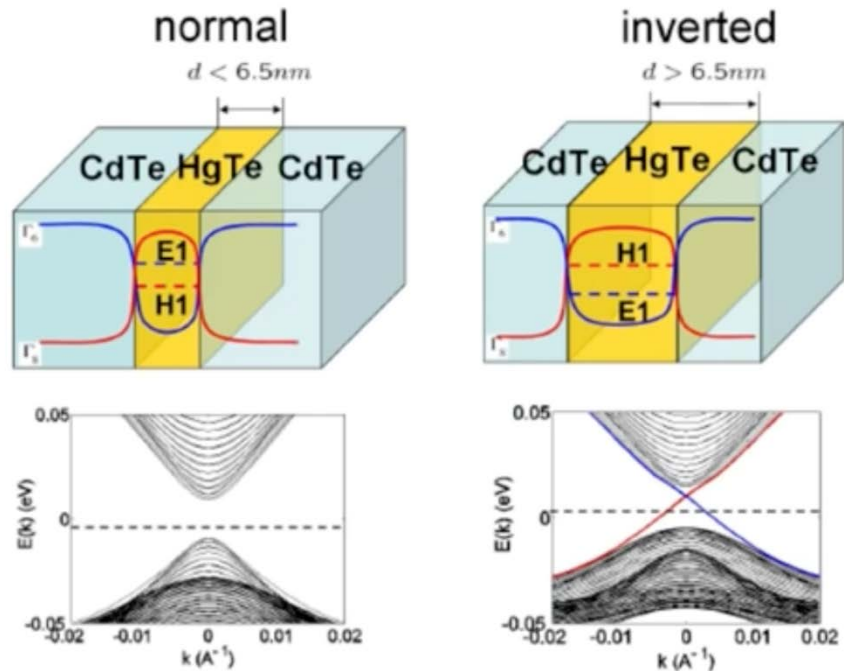
Tight-binding model: P. R. Wallace, (1947)
(nearest neighbor overlap = γ_0)

$$E(\mathbf{k}) = E_F \pm \gamma_0 \sqrt{1 + 4 \cos\left(\frac{\sqrt{3}k_x a}{2}\right) \cos\left(\frac{k_y a}{2}\right) + 4 \cos^2\left(\frac{k_y a}{2}\right)}$$



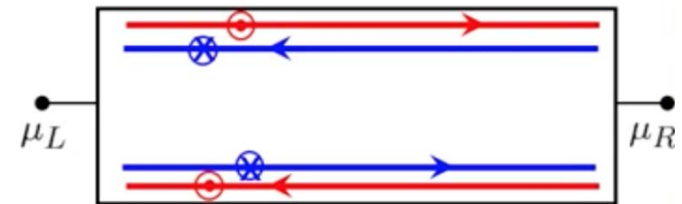
Graphene: Geim, Novoselov et al. PNAS 102, 10341 (2005)

2D TI: Quantum Spin Hall Effect - Experiments

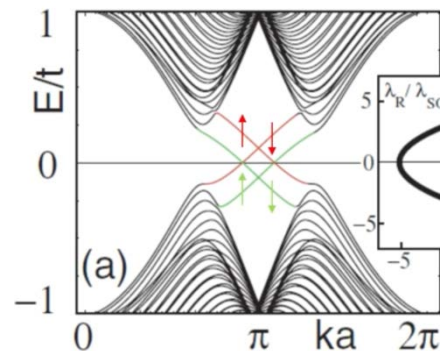


QSHE thought to be ground state of graphene, but SOC too small in graphene

HgTe quantum wells predicted to show QSHE (Bernevig, Zhang 2006)



Perfect (dissipationless) 1D conducting channel



- 1D edge states
- Opposite spins travel in opposite dir.
- TRS
- Two copies of Haldane model
- Topological Z2 invariant: only 2 types of TRS 2D insulators

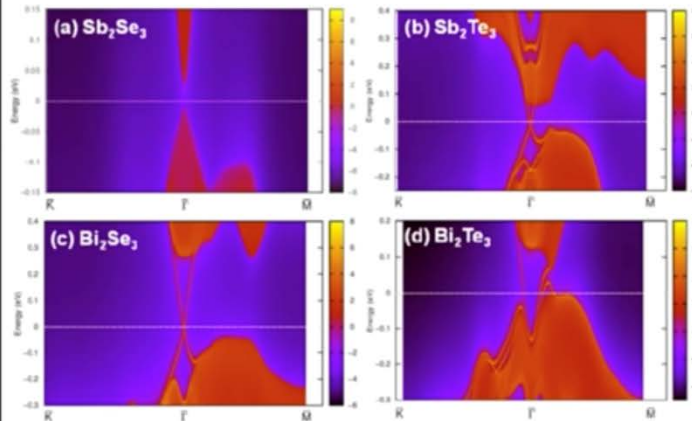
3D TIs: From Theory to Experiments

Theory

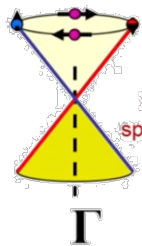
Topological insulators in Bi_2Se_3 , Bi_2Te_3 and Sb_2Te_3 with a single Dirac cone on the surface

Haijun Zhang¹, Chao-Xing Liu², Xiao-Liang Qi³, Xi Dai¹, Zhong Fang¹ and Shou-Cheng Zhang^{3*}

DFT calculation



Zhang *et al.*, Nature Physics, 5, 438 (2009)

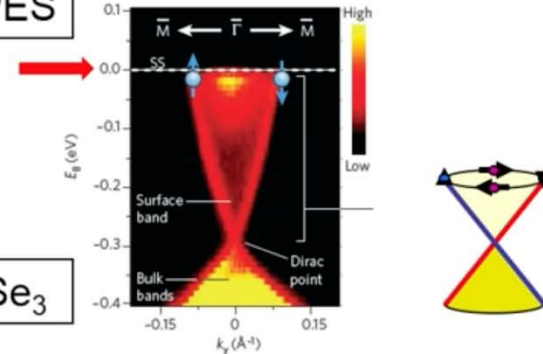


2D surface state
with Dirac dispersion
spin-momentum coupling

Fu, Kane, Mele PRL 2005
Moore, Balents PRB 2005
Roy PRB 2009

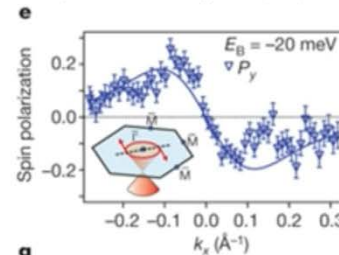
Experiment

ARPES



Bi_2Se_3

Xia *et al.*, Nature Physics, 5, 398 (2009)



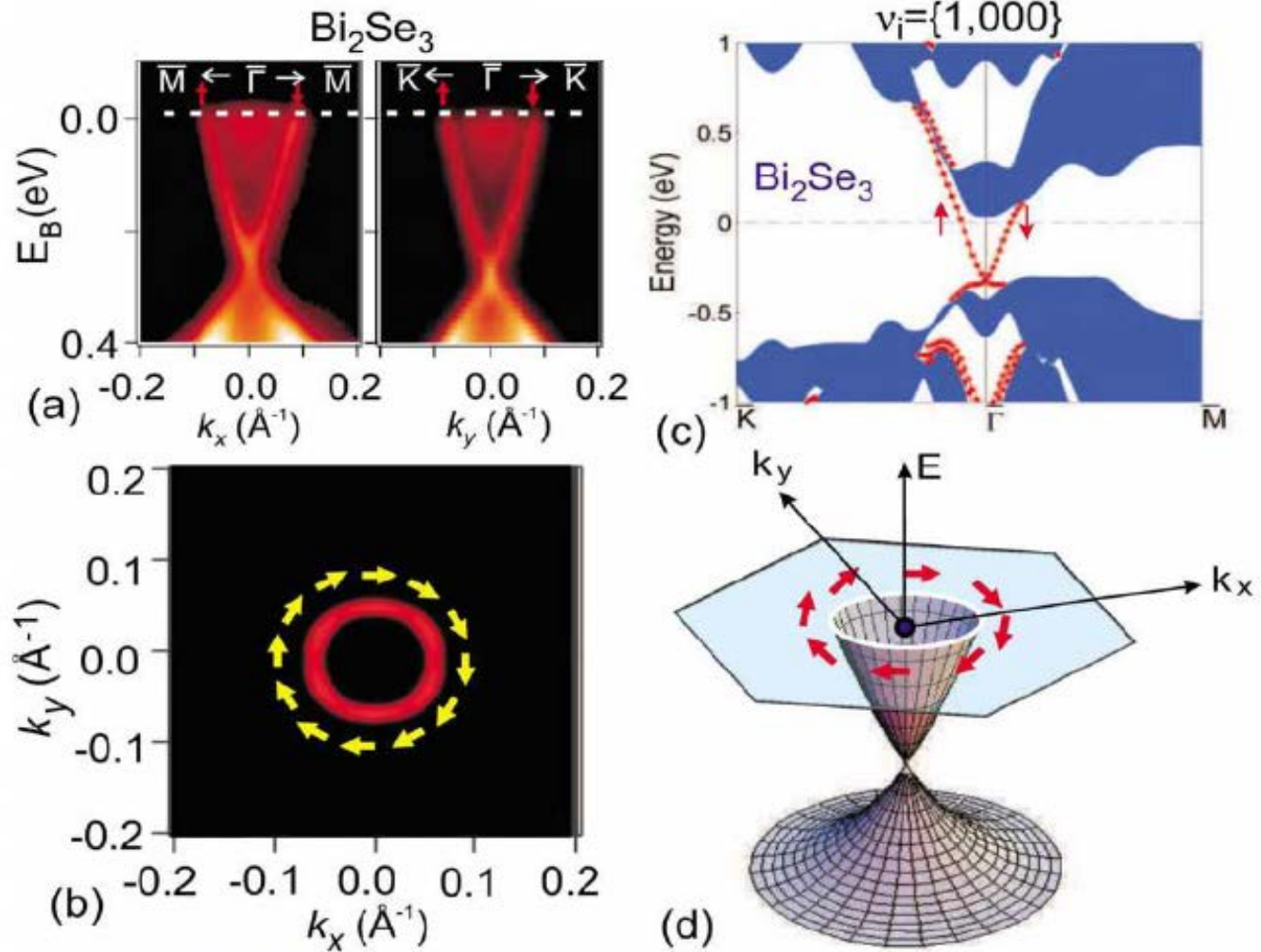
Hsieh, Hasan *et al.*, Nature, 460, 1101 (2009)

4 Z_2 invariants in 3D:

$\nu_0; (\nu_1, \nu_2, \nu_3)$

$\nu_0=1$: strong TI

$\nu_0=0, (\nu_1, \nu_2, \nu_3)$ not all 0:
Weak TI (stacked 2D TIs)

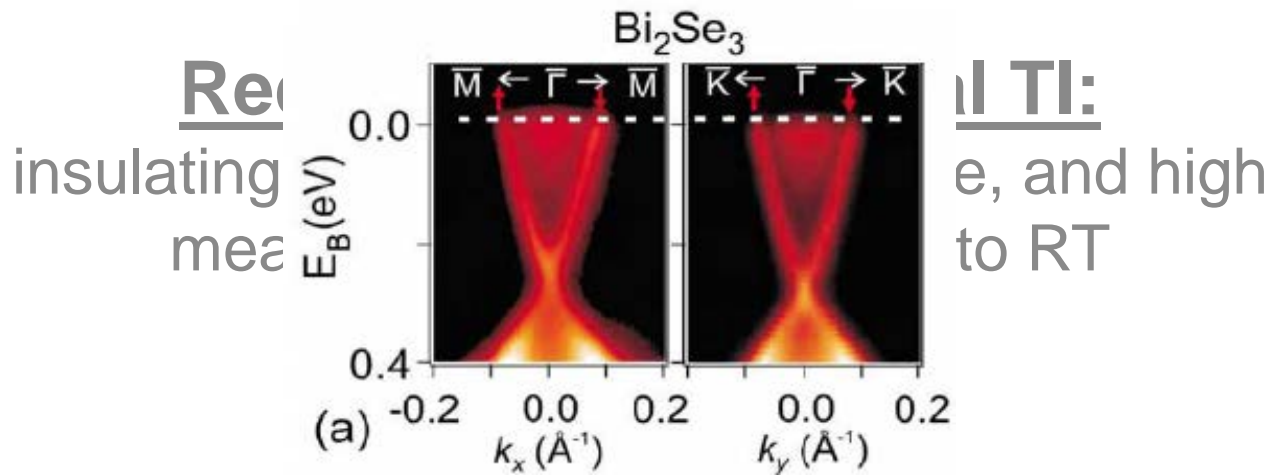


NATURE PHYSICS | VOL 5 | JUNE 2009 |

Prediction: Kane, Mele, Fu (PRL 2005, 2007), Bernevig et al. (Science 2006).
Experimental observation: 2D: HgCdTe QWs (König 2007), 3D: Bi_{1-x}Sb_x (Hsieh 2008), Bi₂Se₃ (Xia 2009)

Characterization Techniques:

ARPES, STM, transport, etc. **mixed bulk & surface contributions**



n-type vs p-type

Goal: Probe n - and p -Type Materials, With Defects, up to RT

selectivity to bulk vs surface

non-ideal materials, defects

NMR reports on carrier concentration density of states, magnetic order, effective mass, etc.

nanoscale resolution

heterostructures, interfaces

TODAY'S TOPICS

Topological band structures

Topological Insulators

Topological Crystalline Insulators

Dirac Semimetals

TI BULK PROPERTIES

As Probed by Conventional SS-NMR

Bulk Defects

Phase Separation

Electronic Homogeneity

Carrier conc. & Type, *p*-to-*n* Transition

Band Inversion

Adv. Electr. Mater. 1, 1500117 (2015); APL Materials 3, 083601 (2015); Phys. Rev. B 90, 125201 (2014); Adv. Func. Mater. 24, 1519-1528 (2014); J. Phys. Chem. C 117, 8959-8967 (2013); J. Phys. Chem. C 116, 17300-17305 (2013)

E-N Hyperfine Interaction

$$H_D = -2\mu_B\gamma_n\hbar\mathbf{I} \cdot \left[\frac{\mathbf{1}}{r^3} - \frac{3\mathbf{r}\mathbf{r}}{r^5} \right] \cdot \mathbf{S} \quad H_O = -\gamma_n\hbar\frac{e}{mc} \frac{\mathbf{I} \cdot (\mathbf{r} \times \mathbf{p})}{r^3}$$

$$H = H_Z + H_Q + \{H_F + H_D + H_O\}$$

$$\|H_Z\| \gg \|H_Q\| \gg \|H_D\|, \|H_O\|$$

$$H_Z = -\gamma\hbar B_0 \sum_i I_{z,i}$$

$$H_F = 2 \left(\frac{8\pi}{3} \right) \mu_B\gamma_n\hbar\mathbf{I} \cdot \mathbf{S}\delta(\mathbf{r})$$

$$H_Q = \frac{e^2qQ}{4I(2I-1)} \left[3I_z^2 - \vec{I}^2 + \frac{1}{2}\eta(I_+^2 + I_-^2) \right]$$

Spin dynamics

$$\frac{1}{T_1} = \left(64 \frac{\pi^3}{9} \right) \gamma_e^2 \gamma_{Li}^2 \hbar^3 \langle |\Psi_k(0)|^2 |\Psi_{k'}(0)|^2 \rangle_F N_{s,p}(E_F)^2 k_B T$$

Knight Shift

$$\frac{1}{T_1} \propto (m_e^*)^2 n_e^{\frac{2}{3}} kT$$

Fermi-Dirac

$$\frac{1}{T_1} \propto (m_e^*)^{\frac{3}{2}} n_e (kT)^{\frac{1}{2}}$$

Maxwell-Boltzmann

$$K = \zeta \left(\frac{8\pi}{3} \right) \gamma_e^2 h^2 \langle |u_{k(0)}|^2 \rangle_{E_0} \left(\frac{n_e}{kT} \right)$$

Orbital Hyperfine Interaction (TI)

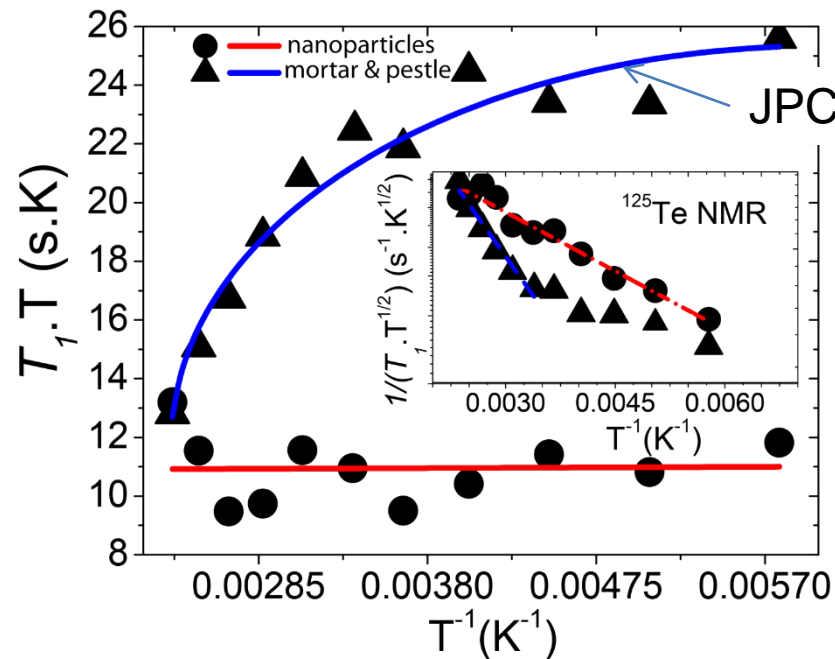
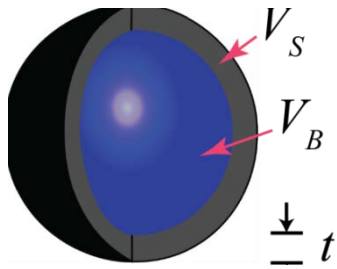
$$H_O \sim \frac{\mathbf{I} \cdot (\mathbf{r} \times \mathbf{p})}{r^3} \quad H_O^{(TI)} \sim \frac{\mathbf{I} \cdot (\mathbf{r} \times v_F \boldsymbol{\sigma})}{r^3}$$

$v_F \sim 5 \cdot 10^5$ m/s or ~ 0.7 eV
vs 10^{-6} eV for usual HFI

(nucleus interacts with orbital motion of Dirac electron)

KORRINGA LAW IN Bi_2Te_3

First Time Observed in a TI



JPCC 116, 17300 (2012)

NEGATIVE KNIGHT SHIFT

First Time Observed in a TI

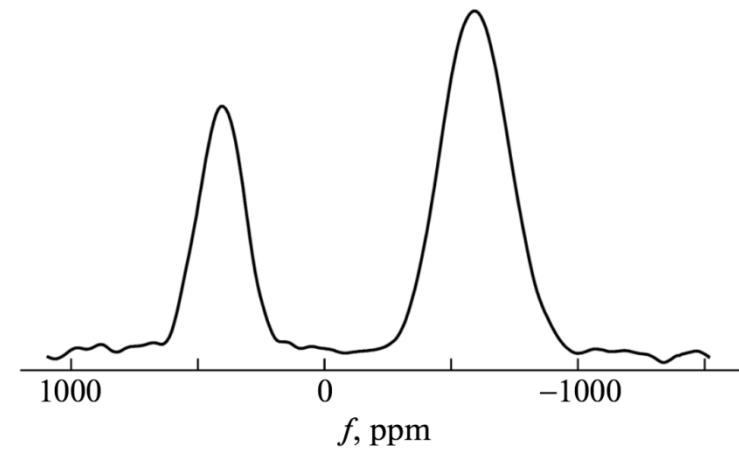
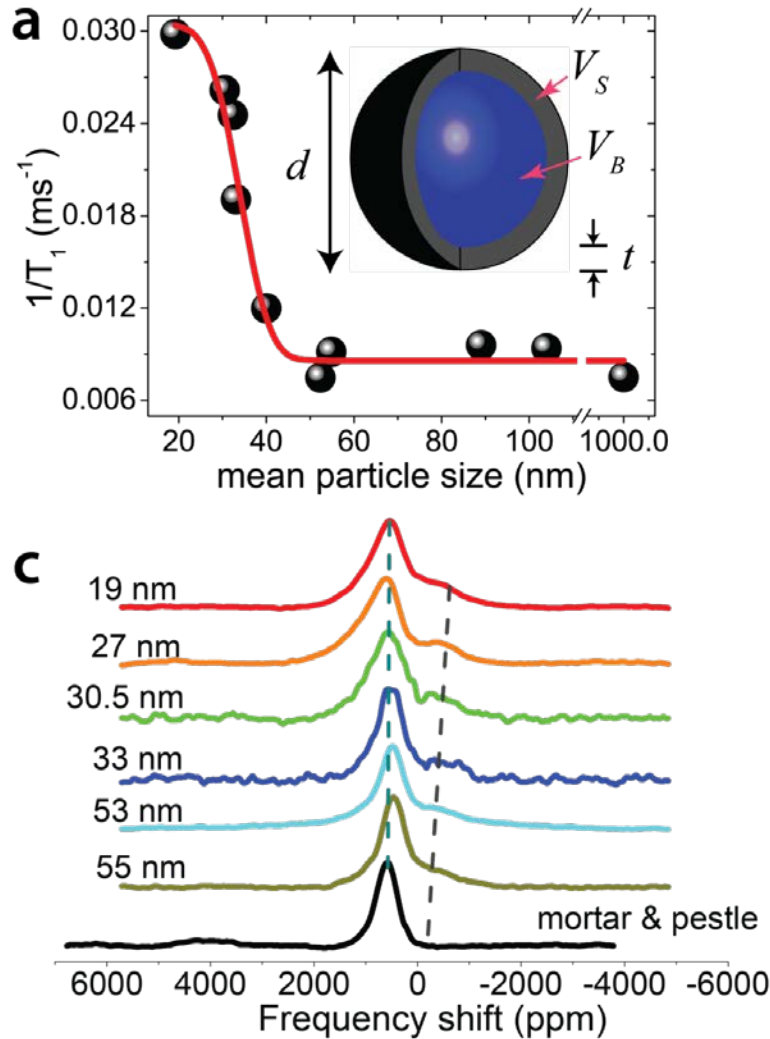


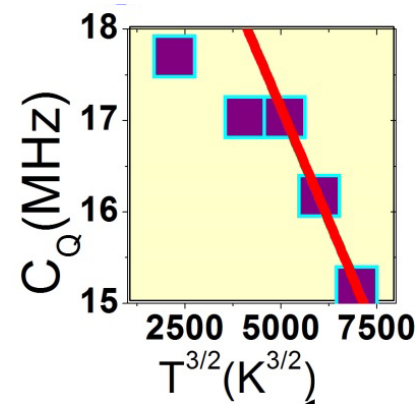
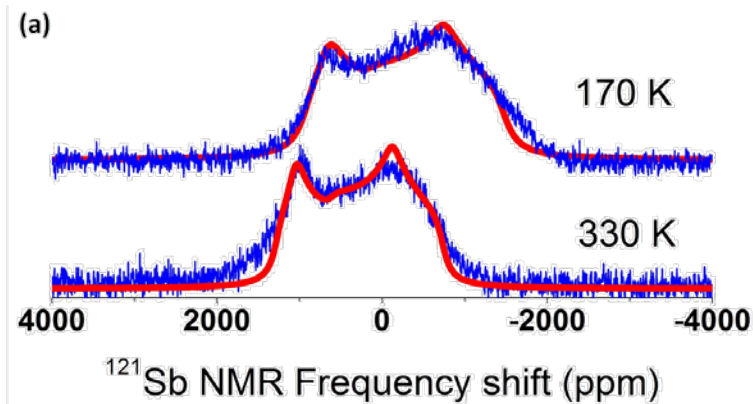
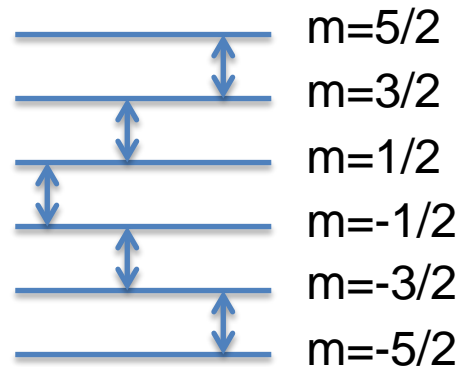
Fig. 1. ^{125}Te NMR spectrum of Bi_2Te_3 single crystal at room temperature. The c axis of the crystal is directed along the external magnetic field.

Podorozhkin, et al., Phys. Solid State 57, 1741 (2015)

Nuclear Quadrupolar Central Transition

^{121}Sb nuclei
($I=5/2$)

$$H_Q = \mathbf{I} \cdot \overleftrightarrow{Q} \cdot \mathbf{I}$$



^{121}Sb vs T for Sb_2Te_3

Isotopic Ratio & Korringa Law

magnetic relaxation mechanism

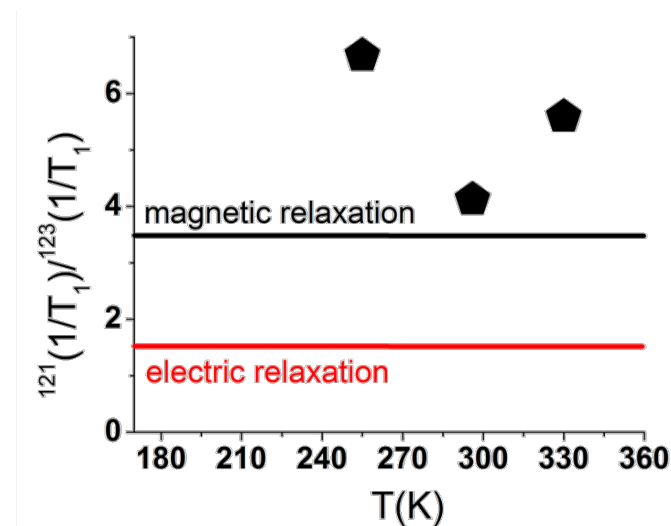
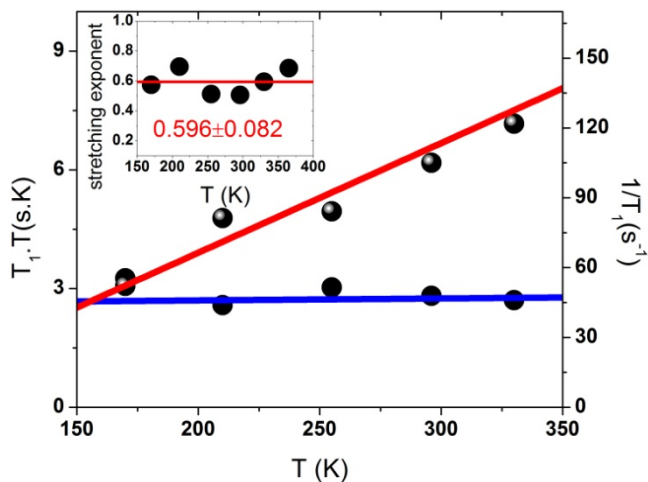
^{121}Sb nuclei ($I=5/2$)

$$\frac{{}^{121}(\frac{1}{T_1})}{{}^{123}(\frac{1}{T_1})} = \frac{{}^{121}\gamma_n^2}{{}^{123}\gamma_n^2} = 3.41$$

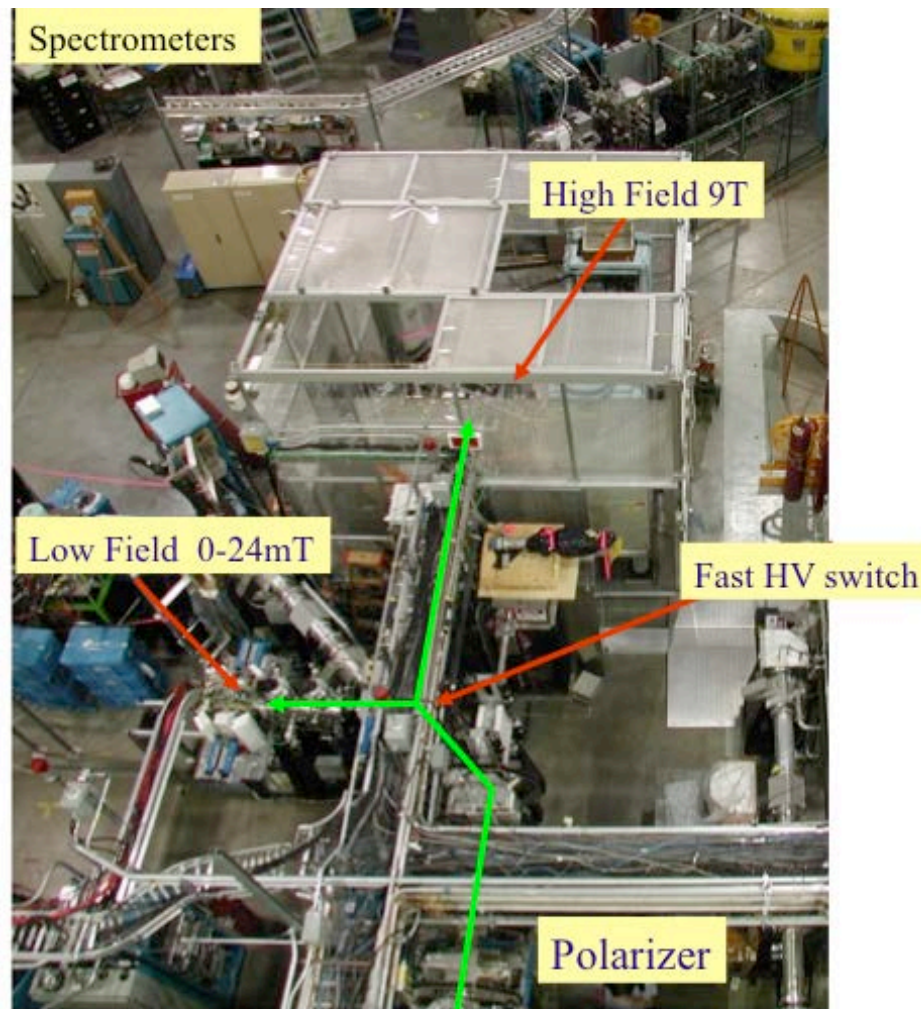
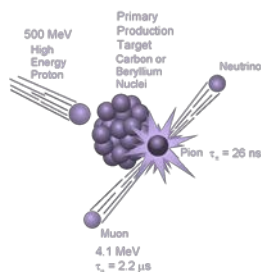
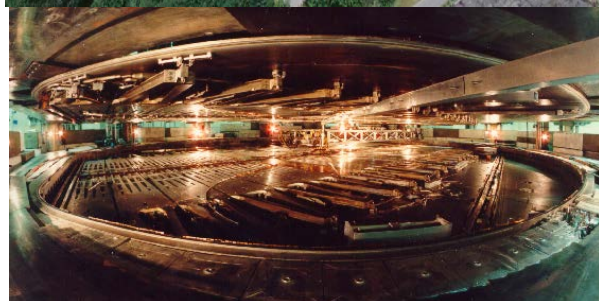
^{123}Sb nuclei ($I=7/2$)

electric relaxation mechanism

$$\frac{{}^{121}(\frac{1}{T_1})}{{}^{123}(\frac{1}{T_1})} = \frac{({}^{121}q)^2 \times \frac{(2I+3)}{I^2(2I+1)}}{({}^{123}q)^2 \times \frac{(2I+3)}{I^2(2I+1)}} = 1.44$$



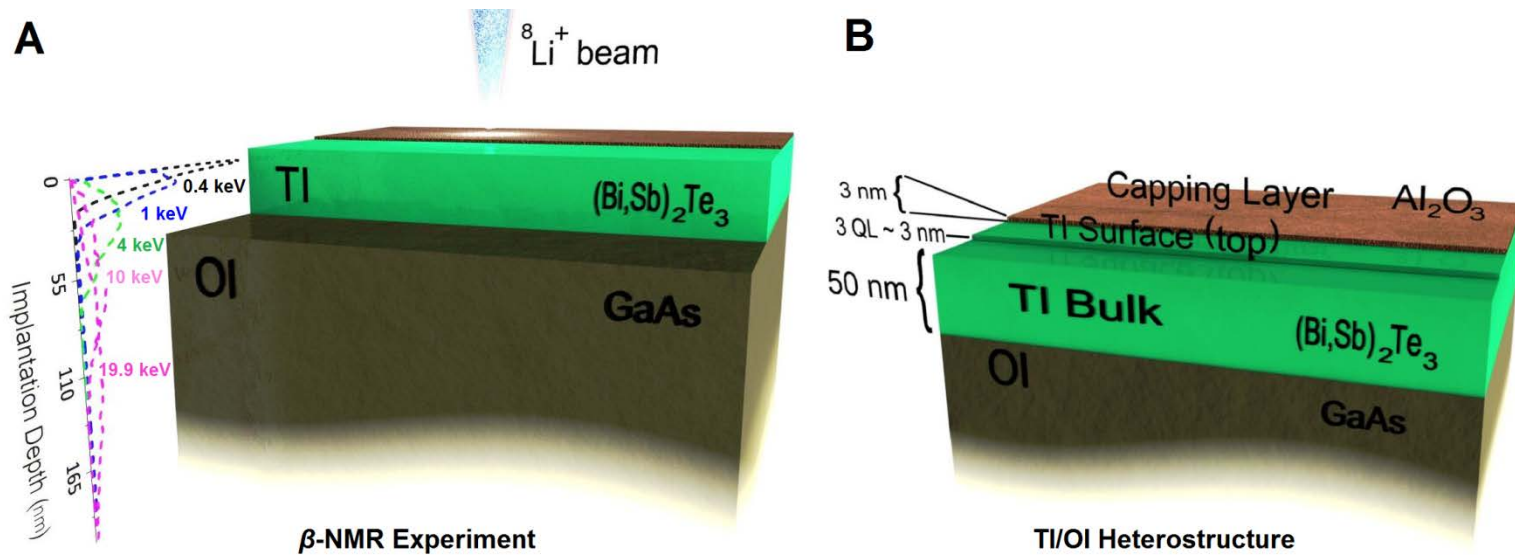
β NMR STUDIES @ ISAC-I Facility, TRIUMF



NMR μ SR β -NMR

Polarization	<0.01		>0.8
detection method	electronic pickup		anisotropic β decay
Sensitivity	10^{17} spins		10^7 spins
T_1 range (s)	$10^{-5} - 10^{-2}$	$10^{-8} - 10^{-4}$	$10^{-3} - 10^{-3}$
range	N/A		
0.5 mm	$10 \text{ \AA} - 3000 \text{ \AA}^*$		
Applied field	high	any	small-high

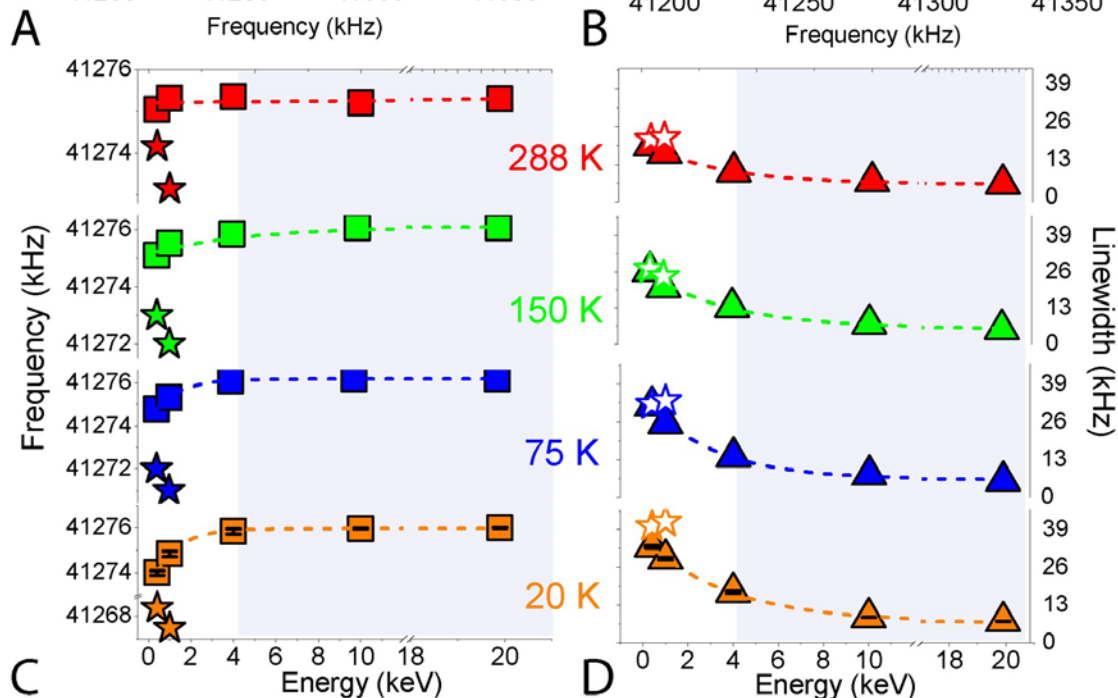
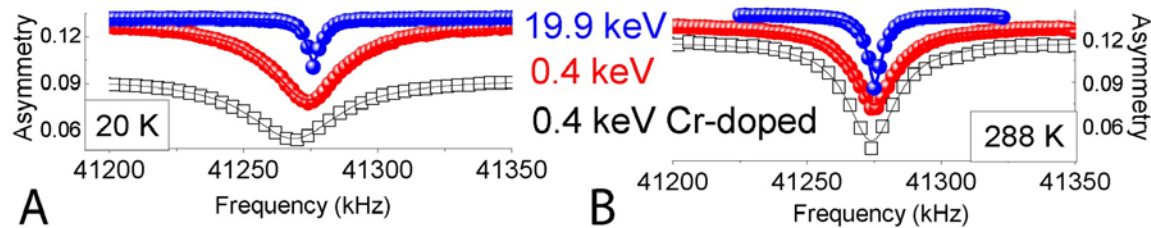
M1352: TI/OI Thin-Film Heterostructure



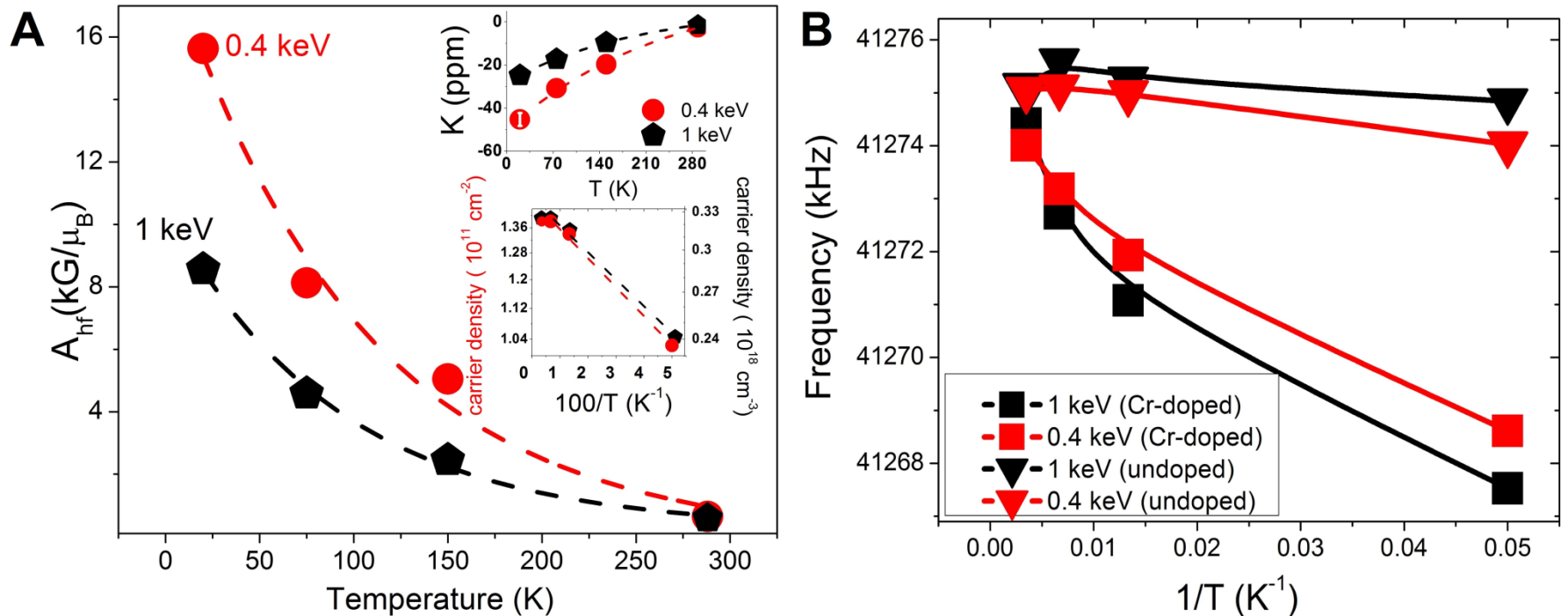
0.4 keV, 50% signal originates from TI surface, $d=4$ 3 nm
1 keV, 80% originates from TI bulk

Knight Shift Measures Carrier Density, s-o Mixing, Density of States @ E_F

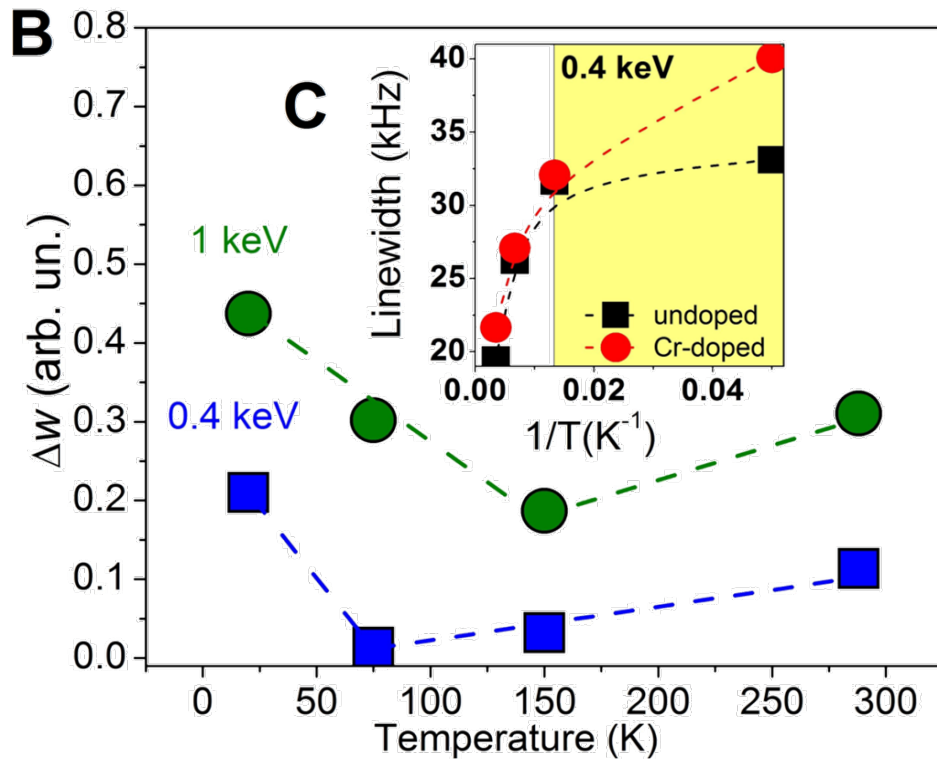
$$K = \frac{4\pi}{3} g \cdot g^* \cdot \mu_B^2 \cdot \langle |u_k(0)|^2 \rangle_{E_0} \rho(E_F) \quad (\cos^2 \theta^+) \langle R | \Delta(\mathbf{r}) | R \rangle$$



M1352: Knight Shift, Hyperfine Constant, Local Carrier Concentration



Depth-Resolved Magnetic Properties



$$\Delta w = \frac{W_{CrTI} - W_{TI}}{W_{TI}}$$

$$\frac{W_{CrTI} - W_{TI}}{W_{TI}} = \left(\frac{Jp^2C}{3gk_B} \right) \cdot \frac{1}{T} + D$$

p effective number of Bohr magnetons
 C atomic fraction of paramagnetic atoms
 D temperature independent term
 g electron g -factor
 J effective s - d exchange integral

Nanoscale Findings From Depth Profiling

when going from the bulk to the surface, across a ~10 nm thick layer...

$$T_c^{surface} = 0.5 \cdot T_c^{bulk}$$

$$J^{surface} = 0.9 \cdot J^{bulk}$$

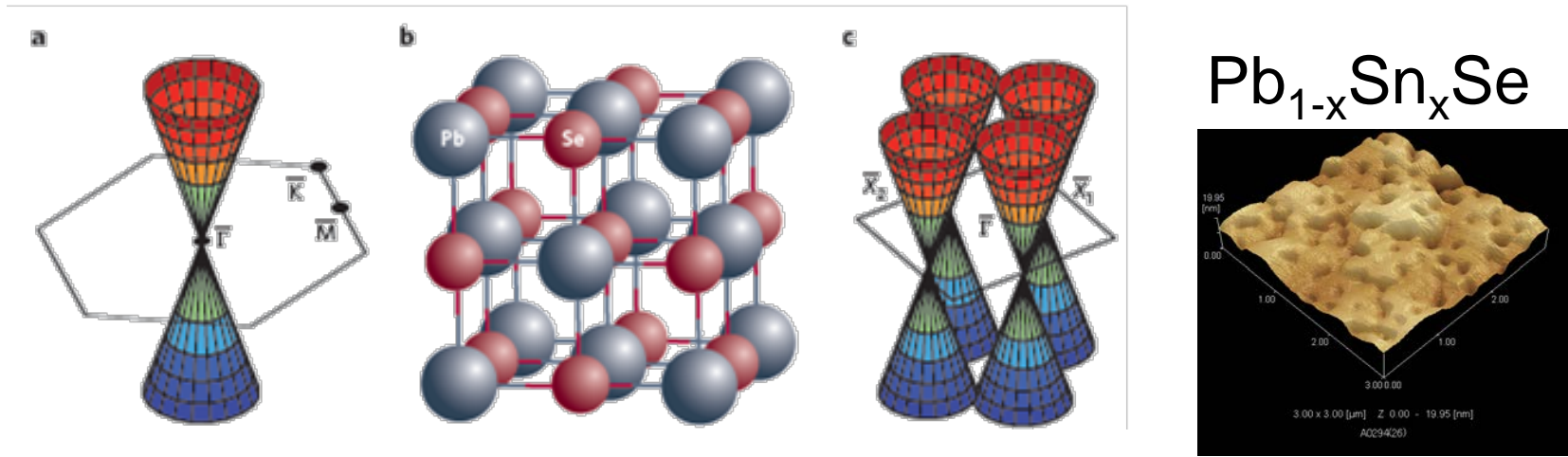
$$n_e^{surface} = 2 \cdot n_e^{bulk}$$

$$A_{hf}^{surface} = 2 \cdot A_{hf}^{bulk}$$

J : effective s - d exchange
integral

TOPOLOGICAL CRYSTALLINE INSULATORS

TCIs Have Even Number Of Dirac Cones



crystalline symmetry replaces time-reversal symmetry

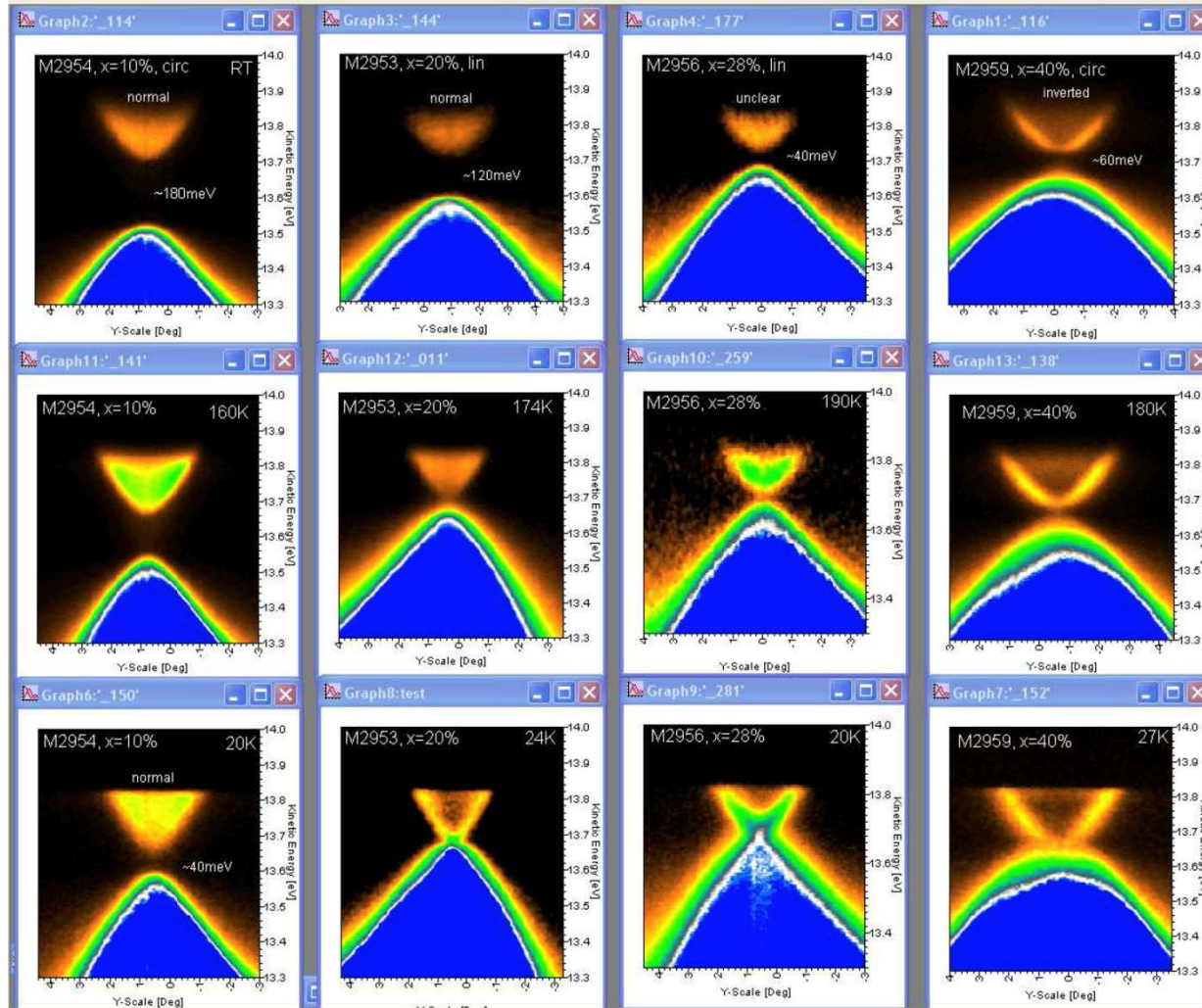
surface states protected by crystal mirror symmetry

only on crystal faces perpendicular to the mirror planes

L. Fu, Phys. Rev. Lett. 106, 106802 (2011); T.H. Hsieh, et al., Nature Comm. 3, 982 (2012).

ARPES of $\text{Pb}_{1-x}\text{Sn}_x\text{Se}$, $x=10-40\%$

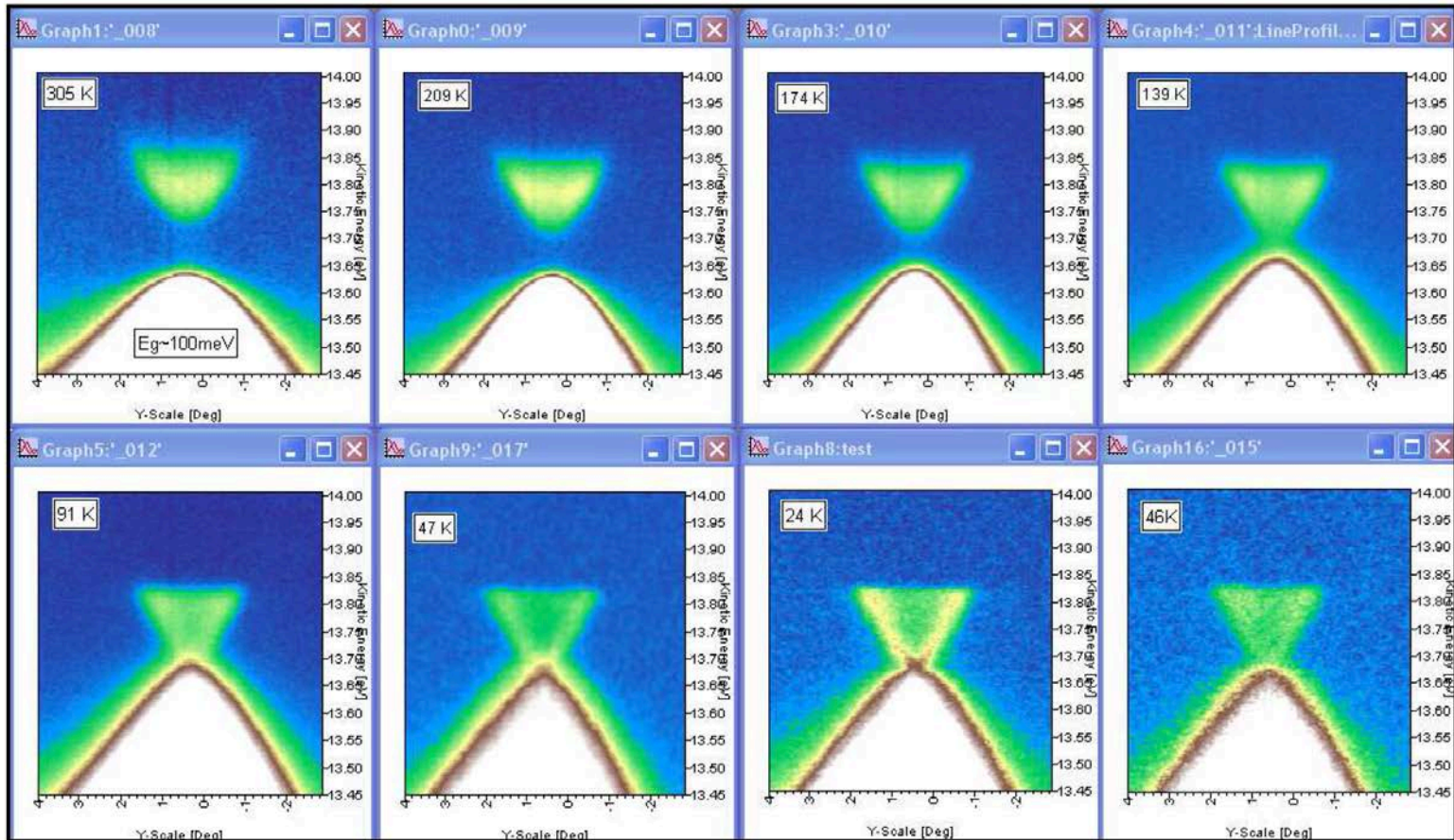
At room temperature (upper row), at $\sim 180\text{K}$ (middle) and at 20K (lower row)



vs T

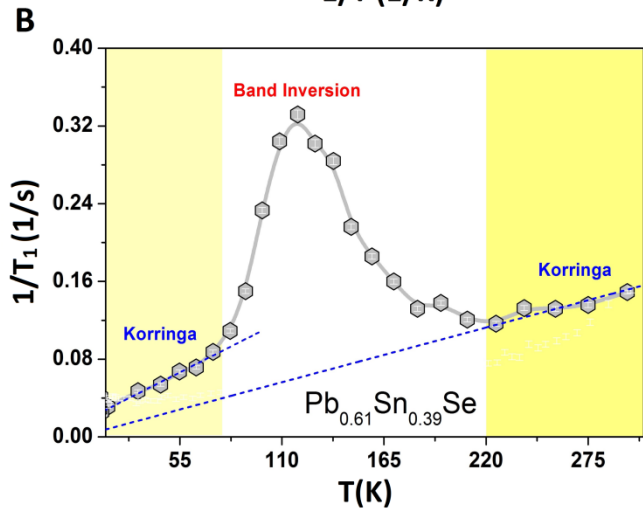
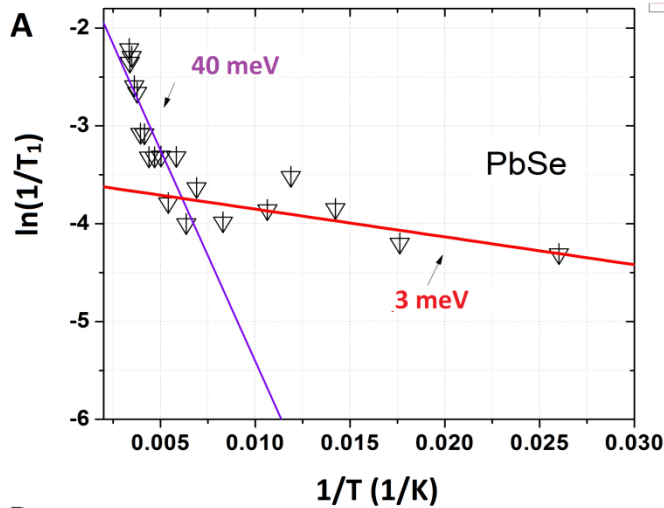
vs doping ($x=0.1, 0.2, 0.3, 0.4$)

CD vs T, $\text{Pb}_{1-x}\text{Sn}_x\text{Se}$, $x=20\%$

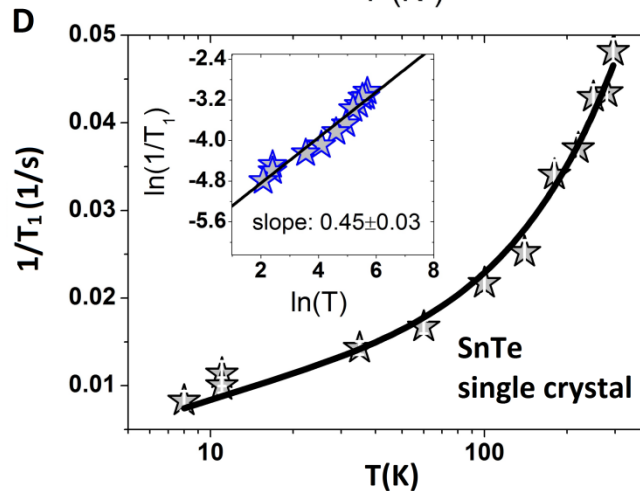
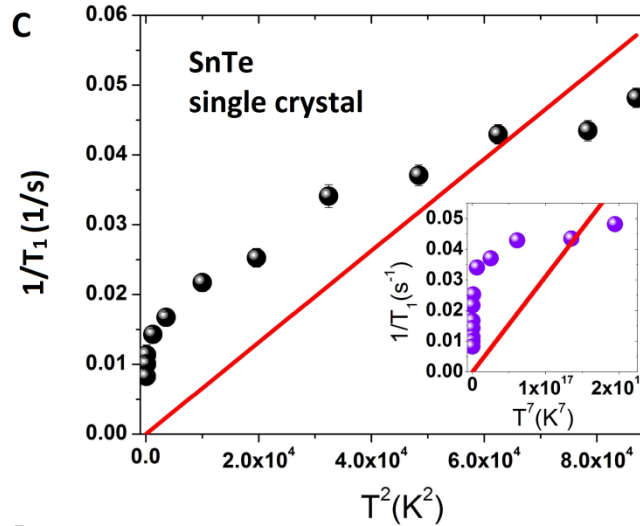


Recall that $\frac{1}{T_1} \propto N_{s,p}(E_F)^2$

Spin Dynamics and BI



Pb_{0.61}Sn_{0.39}Se @ 130K,
drop in resistivity



Ferroelectricity:

Van Kranendonk &
Walker (1968)

$$\frac{1}{T_1} \propto T^2 \text{ for } T \geq \theta_D$$

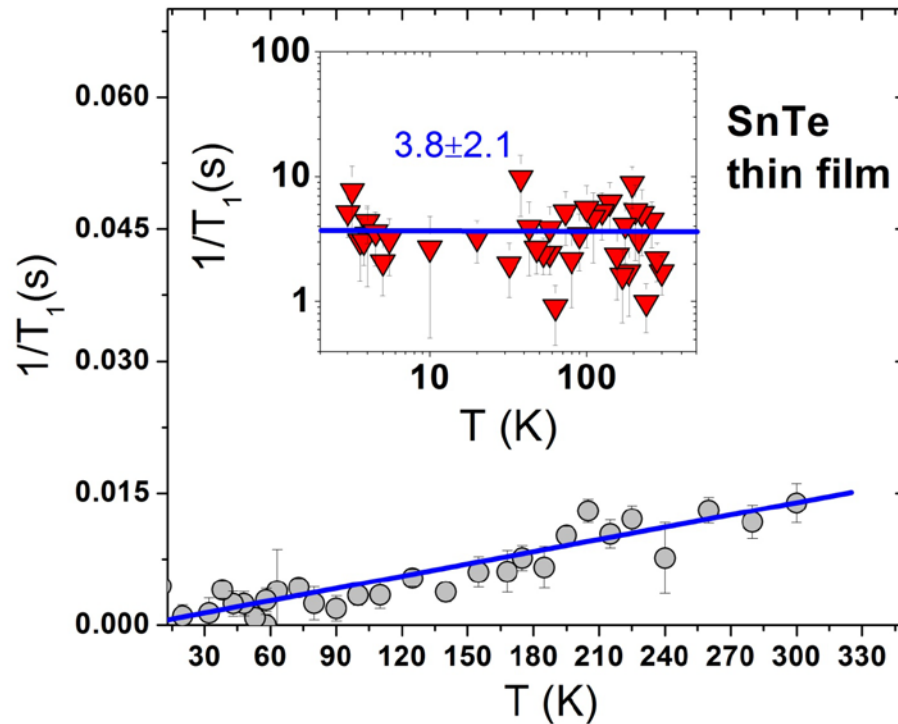
$$\frac{1}{T_1} \propto T^7 \text{ for } T \leq \theta_D$$

$\theta_D \sim 150$ K SnTe

$1/T_1$ expected to
change at $T_c \sim 100$
K (critical slowing
of the soft mode)

$$\frac{1}{T_1 \cdot T} = \frac{1}{T_{1K} \cdot T} + C \cdot T \cdot e^{-\frac{\Delta}{k_B T}}$$

Surface State like Conductive Metal

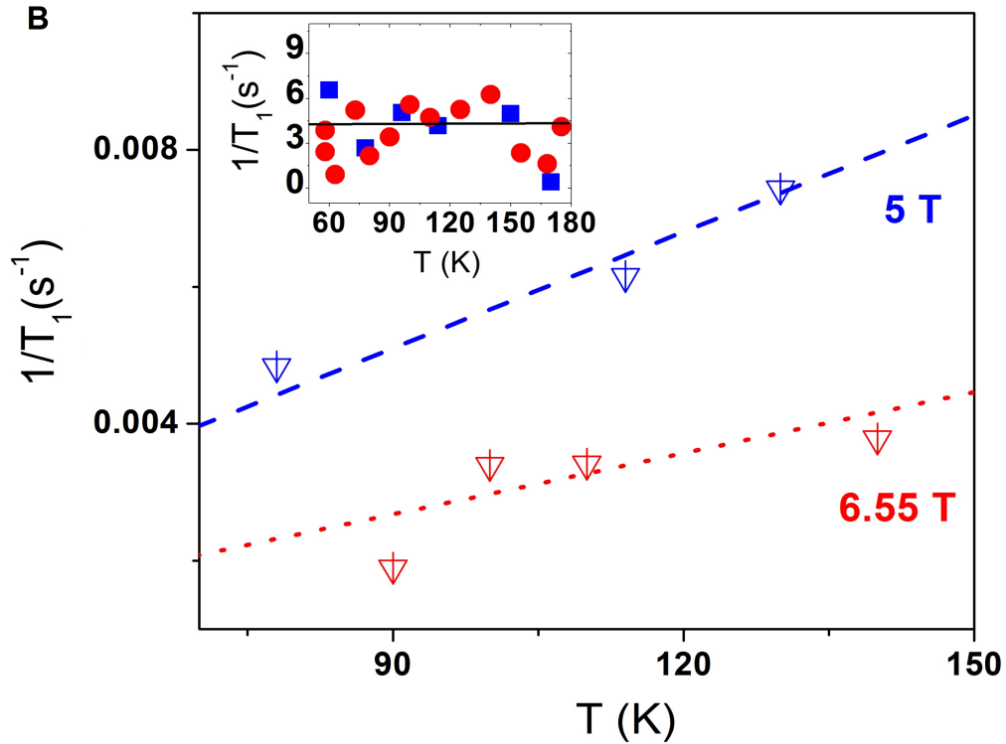


$1/T_1 \cdot T \sim 0.98$ -> highly conductive state (non-interacting carriers, no electron-electron correlations)

SnTe surface is more metallic than Ag or Au

Metallicity hard to detect via volume-averaged readouts

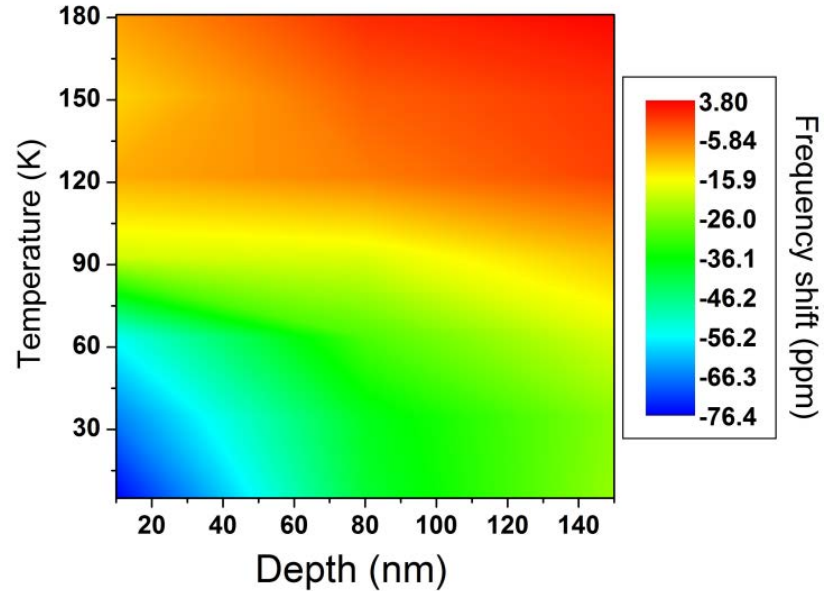
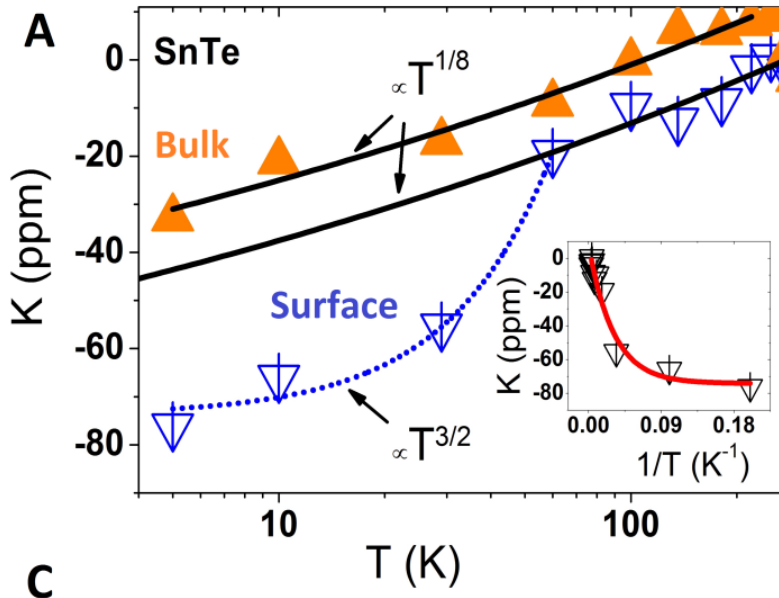
Field-Depending Korringa Process



Field dependence also observed in various quantum Hall systems.

Knight Shift @ Surface Reveal Gapless Semiconductor

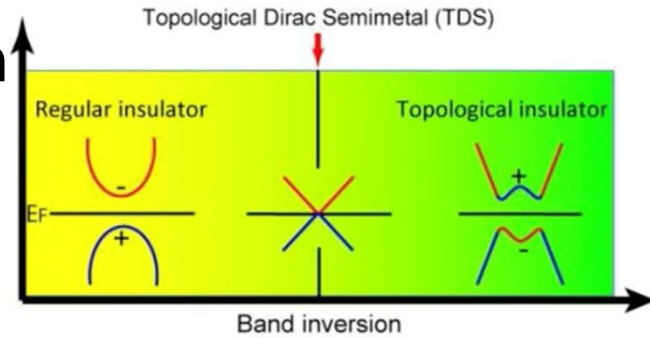
$$K = B \cdot T^n + D$$



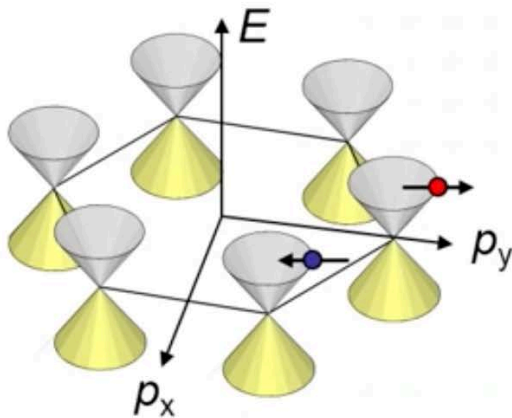
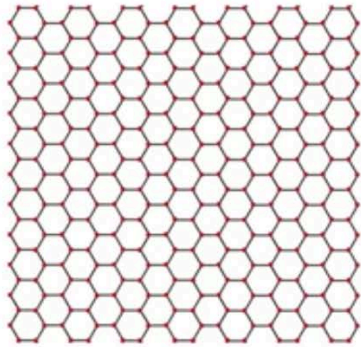
$1/T^{3/2}$ law typical of gapless semiconductors
 (Tsidilkovski 1997, Zhang 2015)
 sub-linear power law ($n < 1$) due to presence of defects and disorder

Topological Dirac Semimetals

TDS lie at a quantum critical point between trivial insulator and TI



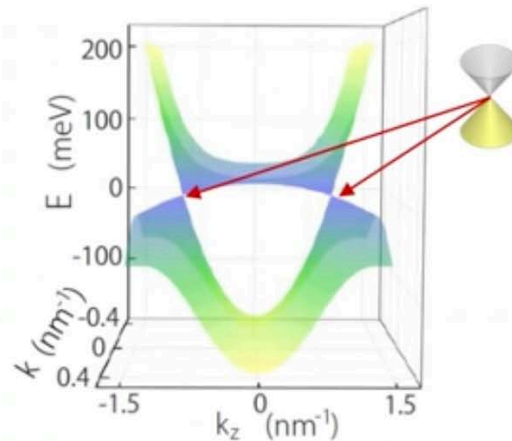
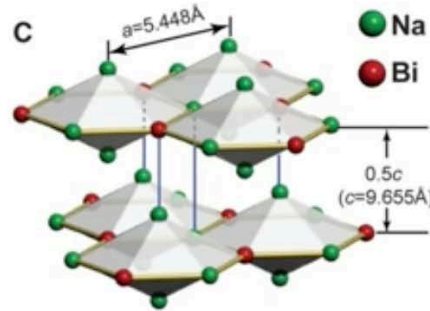
Graphene (2D)



$$H = v_F (\boldsymbol{\sigma} \cdot \mathbf{p})$$

Na₃Bi (3D)

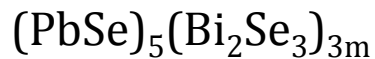
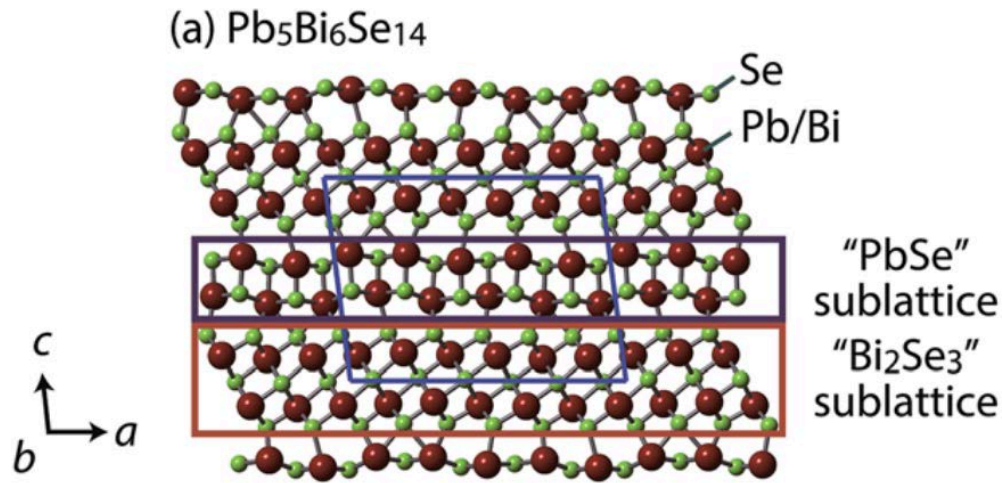
(3D topological Dirac semimetal)



$$H = v_F (\boldsymbol{\sigma} \cdot \mathbf{p})$$

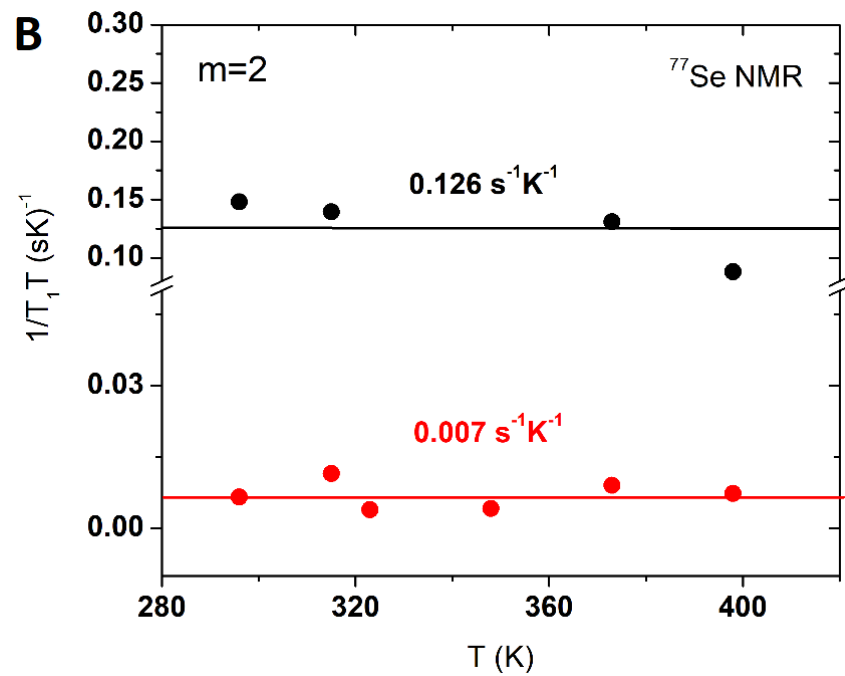
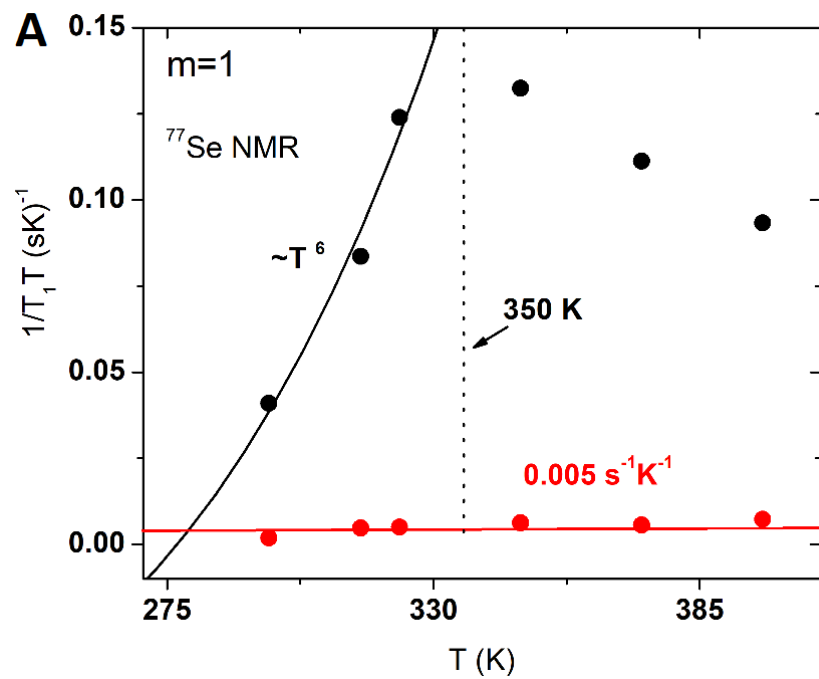
also
Cd₃As₂
ZrTe₅(?)
Others?

Evolution of non-trivial Fermi Surface Features in the Band Structures of $\text{Pb}_5\text{Bi}_6\text{Se}_{14}$ and $\text{Pb}_5\text{Bi}_{12}\text{Se}_{23}$



$m=1$ $\text{Pb}_5\text{Bi}_6\text{Se}_{14}$ semiconducting

$m=2$ $\text{Pb}_5\text{Bi}_{12}\text{Se}_{23}$ semimetallic



SUMMARY

Topological States

TI bulk & surface States near RT, p-type materials,
studies of materials with high defect content

TCIs slightly more complicated because of the band
inversion vs T and x ; no ferroelectric transition in SnTe

Contributors:

D. Koumoulis, J.P. Scheifers, R. Touzani, B.P.T. Fokwa, R.E. Taylor, K.L Wang, L. He, X. Kou, D. King, F. Alkan, C. Dybowski (U Del.), G.D. Morris (TRIUMF), G.A. Fiete (UT Austin), M.G. Kanatzidis (NWU), Thomas Chasapis (NWU), G. Springholz (Linz), R. Akiyama, S. Ishikawa, S. Kuroda (Univ. of Tsukuba)

For More Info See:

Adv. Electr. Mater. 1, 1500117 (2015); Proc. Natl. Acad. Sci. USA 112, E3645-E3650 (2015); APL Materials 3, 083601 (2015); Phys. Rev. B 90, 125201 (2014); Adv. Func. Mater. 24, 1519-1528 (2014); J. Phys. Chem. C 117, 8959-8967 (2013); Phys. Rev. Lett. 110, 026602 (2013); J. Phys. Chem. C 116, 17300-17305 (2013)

ACKNOWLEDGMENTS

